Computers and Chemical Engineering 189 (2024) 108774

Contents lists available at ScienceDirect

Computers and Chemical Engineering

journal homepage: www.elsevier.com/locate/cace

Control-oriented modeling of direct-heat co-current rotary dryers for energy demand flexibility☆

Jan M. Schaßberger *, Lutz Gröll, Veit Hagenmeyer

Karlsruhe Institute of Technology, Institute for Automation and Applied Informatics, Hermann-von-Helmholtz-Platz 1, Eggenstein-Leopoldshafen, 76344, Germany

ARTICLE INFO

Keywords:
Control-oriented modeling
Partial differential–algebraic equation
Co-current rotary dryer
Energy demand flexibility

ABSTRACT

The contribution presents a new control-oriented model for direct-heat co-current rotary dryers with a focus on demand-side flexibility considering the variation of material throughput and heat source. The dryer model is based on partial differential-algebraic equations covering time- and location-dependent gas and particle velocities taking phase interactions into account. In addition, a steady-state model of a heat supply unit covering electricity-based and chemical heat sources is presented. The model is qualitatively compared with measured data and models from literature showing good overall agreement. Furthermore, simulations of the flexibility mechanisms are performed and their effect on temperature and humidity profiles as well as input and output streams of the dryer are analyzed. On this basis, requirements to process control are discussed. The simulations show that the variation of the throughput is associated with significant changes to the gas input stream, while only small changes are observed for the variation of the energy carrier.

1. Introduction

In order to address climate change, greenhouse gas emissions must be reduced causing an ongoing shift from fossil fuels towards renewable sources in the energy sector. However, due to the intermittent nature of many renewables, energy flexibility is required to ensure the stability of the future electrical grid (Cruz et al., 2018). In this context, a particularly important role is attributed to industrial demand-side flexibility (Heffron et al., 2020), i.e. the possibility of industrial processes to increase or decrease their energy demand if required by the grid. For this reason, the flexibility of industrial processes with a large electrical energy demand, like e.g. chlor-alkali electrolysis (Otashu and Baldea, 2019; Weigert et al., 2021), is subject of recent research. Moreover, dynamic operation of processes relying on raw materials that will be produced in the future by means of renewable energy are addressed, as for instance methanol (Leipold et al., 2023) or ammonia (Rosbo et al., 2023) synthesis. However, due the simultaneous decarbonization of the industry by electrification (Wei et al., 2019), industrial processes which were not previously known for their high electrical energy demand will also become relevant for demand-side flexibility. One important example is industrial drying as it accounts for 10–20% of total industrial energy consumption in most developed countries (Tsotsas and Mujumdar, 2012). Within this contribution, we focus on flighted direct-heat co-current rotary dryers as this is a frequently encountered type and at the same time a candidate for the drying stage in the new Belite cement recycling process (Stemmermann et al., 2022) serving as a basis for our considerations.

With the considered dryer type, energy flexibility can be achieved by the variation of the material throughput. However, in most cases it is unfavorable to completely shutdown industrial plants due to production rejects and thermal losses during start-up and shut-down even in a phase of prolonged energy shortage. To overcome this issue, the parallel use of multiple energy sources as a second flexibility mechanism can be an appropriate measure. However, both the variation of the throughput as well as the change of the energy source pose challenges to process control, since despite the provision of flexibility, product requirements must be continuously met. Thus, detailed process models predicting the process dynamics over a wide operating range are needed for the development of new control concepts. The rotary dryer is clearly a distributed parameter system for which so-called late-lumping approaches, i.e. design methods based on the infinite-dimensional system model, are to be preferred. One reason for this is, for example, that the approximation of an infinite-dimensional system model typically requires a finite-dimensional model of high order, which needs to be simplified by model order reduction methods for further use in control engineering. This is associated with a loss of information, interpretability of the system states and problems in the preservation of important system properties (Föllinger, 2016).

☆ This work was supported by the Helmholtz Association under the Innopool Project "Energy Transition and Circular Economy".
* Corresponding author.
E-mail address: jan.schassberger@kit.edu (J.M. Schaßberger).

https://doi.org/10.1016/j.compchemeng.2024.108774
Received 16 June 2023; Received in revised form 1 November 2023; Accepted 16 June 2024
Available online 18 June 2024

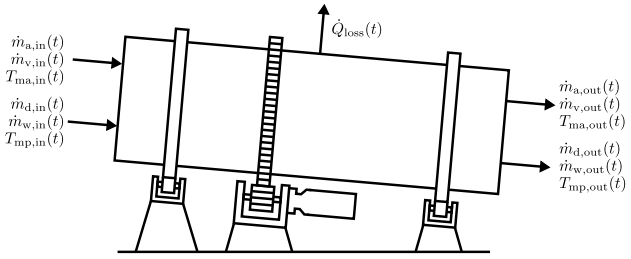

Fig. 1. Scheme of a rotary dryer and its input and output variables: mass flow of moist particles ($\dot{m}_{\mathrm{d}}(t)$, $\dot{m}_{\mathrm{w}}(t)$), moist air ($\dot{m}_{\mathrm{a}}(t)$, $\dot{m}_{\mathrm{v}}(t)$), their temperatures $T_{\mathrm{mp}}(t)$ and $T_{\mathrm{ma}}(t)$ as well as the total amount of heat losses to the environment $\dot{Q}_{\mathrm{loss}}(t)$.

Furthermore, the negligence of parts of the system dynamics in design in general leads to less performing controllers (Deutscher, 2012) and can cause the occurrence of undesirable dynamics or even the instability of the closed control loop (Morris, 2020). Unfortunately, most rotary dryer models are concentrated parameter models (Ortega et al., 2007) or even steady-state only (Arruda et al., 2009). There are few at least partly distributed parameter models based on partial differential equations (PDEs) as in Ajayi (2011) and in Yliniemi (1999). However, the purely distributed parameter models are typically based on strong assumptions such as constant particle and gas velocities and use comparatively simple approaches to model energy and mass transfer, making their suitability for a wide operating range doubtful. Furthermore, there is no model that accounts for the simultaneous use of multiple energy sources. Thus, the main contributions of the present paper are the

- development of a new purely distributed parameter rotary dryer model with increased model depth
- introduction of a new approach for the consideration of spatially distributed velocities as well as the coupled gas-particle transport
- presentation of a heat supply unit model covering electricity-based and chemical energy sources
- discussion of the effects of the mentioned flexibility mechanisms on temperature and humidity profiles in the dryer as well as its input and output streams. On this basis, also requirements on process control are discussed.

The paper is structured as follows. At first, the model of the dryer and the heat supply unit are introduced in Section 2 and Section 3, respectively. Afterwards, a qualitative comparison with results of other models and measurement data from literature is performed in Section 4. Moreover, the effects of the considered flexibility mechanisms and their requirements to process control are discussed. An overview of the nomenclature, subscripts and abbreviations used in the present work is given in Table 3.

2. Rotary dryer model

Fig. 1 shows a scheme of a direct-heat co-current rotary dryer including all process inputs and outputs. At the inlet and outlet, the dryer exchanges material to be dried and hot gas with other process units. For modeling, we consider both flows to be composed of partial flows of dry matter and humidity, i.e., dry particles $\dot{m}_{\mathrm{d}}(t)$ and dry gas $\dot{m}_{\mathrm{a}}(t)$ as well as the related water $\dot{m}_{\mathrm{w}}(t)$ and vapor $\dot{m}_{\mathrm{v}}(t)$. Furthermore, heat losses to the environment occur over the entire dryer length, which are denoted by $\dot{Q}_{\mathrm{loss}}(t)$ in their total amount. For modeling, both the particle and the gas phase are considered to be interacting plug flows, as illustrated in Fig. 2 for an infinitesimal dryer section. In this dryer section, mass $\dot{\mu}_{\mathrm{evap}}(t,x)$ and convective heat transfer $\dot{\gamma}_{\mathrm{conv}}(t,x)$ between the particle and the gas phase are regarded. Moreover, heat loss to the environment $\dot{\gamma}_{\mathrm{loss}}(t,x)$ is taken into account. In difference to

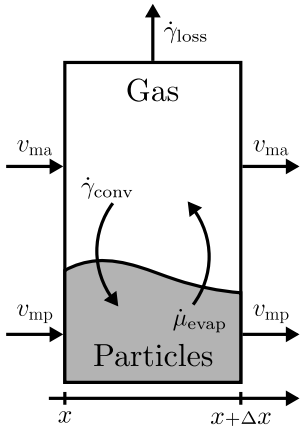

Fig. 2. Material and energy exchange in an infinitesimal dryer section: particle and gas transport over the boundaries with particle velocity $v_{\mathrm{mp}}(t,x)$ and gas velocity $v_{\mathrm{ma}}(t,x)$, heat losses to the environment $\dot{\gamma}_{\mathrm{loss}}(t,x)$ as well as internal material $\dot{\mu}_{\mathrm{evap}}(t,x)$ and heat $\dot{\gamma}_{\mathrm{conv}}(t,x)$ exchange.

existing models, the velocities of the particle phase $v_{\mathrm{mp}}(t,x)$ and the gas phase $v_{\mathrm{ma}}(t,x)$ are considered to be time- and location-dependent.

The remainder of this section is structured as follows. At first the model assumptions are introduced in Section 2.1. Afterwards, the model of the particle phase is presented in Section 2.2 and that of the gas phase in Section 2.3. Afterwards, the approaches to the particle and gas velocity are discussed in Section 2.4 followed by the equations of heat and mass transfer introduced in Section 2.5. Subsequently, the equations used to couple the heat supply unit and the dryer model are introduced in Section 2.6. Finally, the implementation of the presented model is briefly discussed in Section 2.7.

2.1. Dryer model assumptions

The proposed model is derived under the following assumptions

(a) particle and gas phase are modeled by interacting plug flows (Ajayi, 2011; Yliniemi, 1999; Kamke, 1983; Silva et al., 2012)
(b) particle velocity is composed of a time-dependent and a time- and location-dependent part, where the latter is proportional to the local gas velocity (see Section 2.4)
(c) specific volumes of solids and liquids are constant (Ajayi, 2011)
(d) properties of mixtures are determined using linear mixing rules (Didriksen, 2002; Yliniemi, 1999; Rousselet and Dhir, 2016)
(e) kinetic and potential energy of gas and particles are negligible (Ajayi, 2011; Rastikian et al., 1999; Yliniemi, 1999; Didriksen, 2002)
(f) pure species (dry air, water vapor, ...) have constant heat capacities (Didriksen, 2002; Yliniemi, 1999; Silva et al., 2012)
(g) heat capacity of the rotary kiln is negligible (Didriksen, 2002; Yliniemi, 1999; Silva et al., 2012)
(h) heat transfer by radiation is negligible (Castaño et al., 2012; Silva et al., 2012)
(i) pressure inside the dryer is constant (Ajayi, 2011; Kamke, 1983)
(j) unsaturated moist air is treated as a mixture of ideal gases (Didriksen, 2002; Ajayi, 2011; Castaño et al., 2012)
(k) liquid water does not contribute to the volume of the particle phase (Kamke, 1983) (see Section 2.4).

Due to its large heat capacity, the shell of the rotary dryer probably has some influence on the transient behavior of the dryer for changes of the process inputs if they go along with significant changes of the temperature profiles inside the dryer. However, since considering the shell only by means of heat losses is a standard assumption (Didriksen, 2002; Silva et al., 2012), we focus in the present contribution on

the processes inside the shell. In addition to the assumptions, we introduce the following conventions. We use T as symbol for the temperature in degree Celsius and choose 0 °C as reference point for energy considerations without loss of generality. Moreover, we only regard process conditions for which no saturation with regard to the state variables of the PDEs and no condensation of gaseous water occurs such that saturation terms can be neglected from the equations for clarity. However, this does not apply to saturation effects in the equations of heat and mass transfer.

2.2. Particle phase

The particle phase consists of dry particles and liquid water. For modeling, a separate PDE is introduced for each component using the linear mass density of the dry matter $\xi_\mathrm{d}(t,x)$ and water $\xi_\mathrm{w}(t,x)$ as state variables for $t \geq t_0$ and $x \in [0, \ell]$. When considering the mass balance of dry solids in an infinitesimal dryer section, as shown in Fig. 2, one can derive the following PDE with initial condition (IC) and boundary condition (BC) under the mentioned assumptions (a), (b)

$$\begin{aligned} &\partial_t \xi_\mathrm{d}(t,x) + \partial_x \left(v_\mathrm{mp}(t,x) \xi_\mathrm{d}(t,x) \right) = 0, \qquad (1a)\\ &\text{IC}: \quad \xi_\mathrm{d}(t_0,x) = \xi_{\mathrm{d},0}(x),\\ &\text{BC}: \quad \xi_\mathrm{d}(t,0) = \dot{m}_{\mathrm{d,in}}(t)/v_\mathrm{mp}(t,0). \end{aligned}$$

Analogously, the mass density of water contained in the particles is given by

$$\begin{aligned} &\partial_t \xi_\mathrm{w}(t,x) + \partial_x \left(v_\mathrm{mp}(t,x) \xi_\mathrm{w}(t,x) \right) = -\dot{\mu}_\mathrm{evap}(t,x), \qquad (1b)\\ &\text{IC}: \quad \xi_\mathrm{w}(t_0,x) = \xi_{\mathrm{w},0}(x),\\ &\text{BC}: \quad \xi_\mathrm{w}(t,0) = \dot{m}_{\mathrm{w,in}}(t)/v_\mathrm{mp}(t,0). \end{aligned}$$

The previous equations can be read as follows: dry particles and their attached moisture travel with the same varying velocity through the dryer, where the mass density of the moisture reduces continuously due to evaporation. Since the particle velocity is considered to be both a function of time and location, not only the derivative of the local mass densities but also that of the velocity w.r.t. the spatial coordinate contributes to the change of the local dry matter and water density. To model the mass and heat transfer, a PDE for the particle temperature $T_\mathrm{mp}(t,x)$ is derived from the energy balance of an infinitesimal dryer section based on the first law of thermodynamics for a transient open system. When considering assumptions (a)–(h), the energy balance can be rewritten as a PDE for the particle temperature given by

$$\begin{aligned} &\partial_t T_\mathrm{mp}(t,x) + v_\mathrm{mp}(t,x) \partial_x T_\mathrm{mp}(t,x) = \big(\dot{\gamma}_\mathrm{conv}(t,x)\\ &\quad - \dot{\mu}_\mathrm{evap}(t,x) \Delta h_\mathrm{v}(t,x) \big) \,/\, \left(c_\mathrm{d} \xi_\mathrm{d}(t,x) + c_\mathrm{w} \xi_\mathrm{w}(t,x) \right), \qquad (1c)\\ &\text{IC}: \quad T_\mathrm{mp}(t_0,x) = T_{\mathrm{mp},0}(x),\\ &\text{BC}: \quad T_\mathrm{mp}(t,0) = T_{\mathrm{mp,in}}(t), \end{aligned}$$

where c is the specific heat capacity and $\Delta h_\mathrm{v}(t,x)$ the heat of evaporation. The right side of the equation represents the change in temperature given by the quotient of the total transferred heat and the heat capacity of the moist particles. Contrary to intuition, the numerator includes only the heat transfer by convection and the heat of evaporation but not the overall amount of energy related to the mass transfer, which is reasonable as the temperature is an intensive thermodynamic property.

2.3. Gas phase

Similarly to the particle phase, the dry gas and the water vapor are modeled using two transport PDEs defined on $t \geq t_0$ and $x \in [0, \ell]$. With the assumptions (a), (b), one obtains for the mass density of dry air $\xi_\mathrm{a}(t,x)$

$$\begin{aligned} &\partial_t \xi_\mathrm{a}(t,x) + \partial_x \left(v_\mathrm{ma}(t,x) \xi_\mathrm{a}(t,x) \right) = 0, \qquad (2a)\\ &\text{IC}: \quad \xi_\mathrm{a}(t_0,x) = \xi_{\mathrm{a},0}(x),\\ &\text{BC}: \quad \xi_\mathrm{a}(t,0) = \dot{m}_{\mathrm{a,in}}(t)/v_\mathrm{ma}(t,0), \end{aligned}$$

and for the mass density of vapor $\xi_\mathrm{v}(t,x)$

$$\begin{aligned} &\partial_t \xi_\mathrm{v}(t,x) + \partial_x \left(v_\mathrm{ma}(t,x) \xi_\mathrm{v}(t,x) \right) = \dot{\mu}_\mathrm{evap}(t,x), \qquad (2b)\\ &\text{IC}: \quad \xi_\mathrm{v}(t_0,x) = \xi_{\mathrm{v},0}(x),\\ &\text{BC}: \quad \xi_\mathrm{v}(t,0) = \dot{m}_{\mathrm{v,in}}(t,0)/v_\mathrm{ma}(t,0). \end{aligned}$$

For the temperature of the gas phase $T_\mathrm{ma}(t,x)$, the following equation is derived using (a), (b), (d)–(j)

$$\begin{aligned} &\partial_t T_\mathrm{ma}(t,x) + v_\mathrm{ma}(t,x) \partial_x T_\mathrm{ma}(t,x) = \big[-\dot{\gamma}_\mathrm{conv}(t,x) - \dot{\gamma}_\mathrm{loss}(t,x)\\ &\quad + c_\mathrm{p,v} \dot{\mu}_\mathrm{evap}(t,x) \left(T_\mathrm{mp}(t,x) - T_\mathrm{ma}(t,x) \right) \big] / \left(c_\mathrm{p,a} \xi_\mathrm{a}(t,x) + c_\mathrm{p,v} \xi_\mathrm{v}(t,x) \right), \qquad (2c)\\ &\text{IC}: \quad T_\mathrm{ma}(t_0,x) = T_{\mathrm{ma},0}(x),\\ &\text{BC}: \quad T_\mathrm{ma}(t,0) = T_{\mathrm{ma,in}}(t), \end{aligned}$$

where c_p is the specific isobaric heat capacity. The equations for the mass density of dry air and vapor are structurally identical to that of the particles, except for the sign of the mass flow due to evaporation in (2b). This is also true for the temperature PDE, where only the numerator structurally differs from (1c). The differences lie in the additional term for the heat transfer to the environment and the term related to the mass transfer through evaporation. The latter can be explained as follows. After evaporation of the liquid water, the newly formed vapor is still at particle temperature, which is why the gas temperature reduces.

2.4. Particle and gas velocity

Particle transport inside rotary dryers is a complex process as several mechanisms contribute to particle movement (Mujumdar, 2007; Delele et al., 2015)

- Kiln action:
  motion of the particles in the lower half of the shell due to sliding
- Cascade action:
  transport by the flights, falling after discharge and entrainment by the gas flow
- Bouncing and rolling:
  movement after falling and collision with the material at the bottom of the dryer.

In case of an inclined rotary drum, all these effects, shown in Fig. 3, contribute to the transport of particles through the tube. Common residence time models (Delele et al., 2015) suggest a dependency on the mass flow rate of material to be dried, the drum rotation rate, the angle of inclination and the gas velocity. One can easily see that the gas velocity itself is a complex quantity that varies along the spatial coordinate (Ajayi, 2011), as the gas' specific volume and thus the volume flow reduces with decreasing temperature. However, the increase in the gas' mass, caused by evaporation, partially counteracts the decrease in velocity.

Since strongly varying operating conditions are to be expected due to the flexible plant operation, the modeling of the gas and particle transport is of particular importance. For this reason, we briefly discuss existing approaches in the following focusing on the most sophisticated ones for concentrated as well as distributed parameter models. In general, most models regardless of type focus on mass flow as e.g. in Rousselet and Dhir (2016) or consider both the gas and the particle velocity to be constant over the whole dryer length like in Yliniemi (1999). In this case, the residence time of the particles is calculated using empirical residence time models as a function of the operating conditions. However, in Didriksen (2002) a time- and location-dependent particle and gas velocity is introduced for a concentrated parameter model, where the particle velocity is considered to be a sole function of the gas velocity. The author of Didriksen (2002) suggests a quadratic relation between the velocities, based on

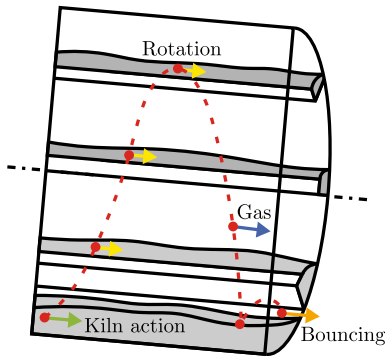

Fig. 3. Particle trajectory and transport mechanisms inside a flighted rotary dryer: kiln action (green arrow), cascade action divided into transport due to rotation (yellow arrow) as well as entrainment by gas (blue arrow) and bouncing (orange arrow).

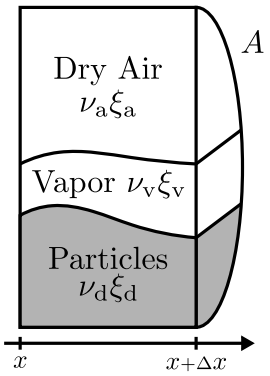

Fig. 4. Illustration of the constraint for an infinitesimal dryer section: the dryer's cross sectional area A is completely occupied by the particles $\nu_d\xi_d(t,x)$, water vapor $\nu_v(t,x)\xi_v(t,x)$ and dry air $\nu_a(t,x)\xi_a(t,x)$.

the assumption of parabolic particle trajectories arising from free falling particles that are accelerated in the horizontal direction by the gas flow. However, the existence of parabolic particle trajectories is questionable due to particle-particle interactions and because of the negligence of the change of the gas velocity w.r.t. the spatial coordinate in the derivation. Usually, even stronger simplifications are made with PDE-based models. In Yliniemi (1999), location independent particle and gas velocities are assumed. Moreover, both velocities are considered to be independent from each other. A more advanced approach is presented in Ajayi (2011) where a time- and location dependent gas velocity is regarded. However, particle velocity is assumed to be constant and no interactions between the particles and the gas w.r.t. velocities are taken into account.

Since the previous approaches for distributed parameter systems do not adequately describe the complex transport processes, a new approach is proposed in this contribution which is in accordance with the theoretical considerations in Baker (1992). We assume that the particle's velocity composes of two components. The first one is a purely time-dependent velocity $v_{rot}(t)$ accounting for the transport of the particles due to drum rotation combined with inclination without influence of the gas stream. Thus, it covers kiln action, lifting by the flights, forward movement during the fall as a result of the drum inclination and the subsequent rolling after the impact on the particle bed. The second component accounts for the additional horizontal movement as a result of the entrainment of the particles by the gas stream during falling and the increased rolling and bouncing distance as a result of the higher velocity with impact of the particles at the bottom of the dryer. Hence, for this component, a dependence on the local gas velocity is considered, where a linear dependency is assumed. This assumption is supported by several residence time models suggesting a linear relation between the gas velocity and the particle residence time (Thibault et al., 2010; Perazzini et al., 2014). Consequently, the particle velocity is given by

$$v_{mp}(t,x) = v_{rot}(t) + k_{vel} v_{ma}(t,x), \tag{3}$$

where $k_{vel} > 0$ is a constant proportionality factor. Both velocity components represent the velocity shares of the individual transport mechanisms perpendicular to the cross-sectional area of the dryer, i.e., the velocity component responsible for the material transport from the inlet to the outlet of the dryer. Both, the proportionality factor and the relation between the particle feed as well as drum rotation rate, for a given inclination of the rotary dryer, need to be estimated from measurement data or determined by experiments.

In order to determine the gas velocity as last remaining PDE state, an algebraic constraint is introduced. At any point (t,x) inside the dryer $x \in [0, \ell]$ for $t \geq t_0$, the dryer's cross sectional area A needs to be filled out completely by the particle and the gas phase as illustrated in Fig. 4. Using the PDE states, their specific volumes ν and the assumptions (c), (d), (j), (k), this condition can be written as follows

$$A \equiv \nu_d\xi_d(t,x) + \nu_a(t,x)\xi_a(t,x) + \nu_v(t,x)\xi_v(t,x). \tag{4}$$

The introduced constraint is independent from the mass density of water since we assume that the liquid water does not occupy additional space as it is located in cracks, etc. of the particles. When considering a material that shrinks significantly while drying, the constraint must be modified appropriately. Since the mass densities of the particles and the moist gas are related via (4), the local velocity is also a function of the mass flow rate of dry solid. This is reasonable, since e.g. an increase of the particle mass flow at constant gas volume flow reduces the cross sectional area so that the gas velocity increases. This is also consistent with the predictions of certain residence time models (Thibault et al., 2010). The PDEs in (1) and (2) form together with the previously introduced constraint (4) and the coupling between the velocities (3) a system of PDAEs, whose implementation is discussed in more detail in Section 2.7.

2.5. Heat and mass transfer

In this section the equations for the mass and energy transfer between the PDEs are described, starting with the heat transfer to the environment in Section 2.5.1. This is followed by the heat and the mass transfer between the phases inside the dryer in Section 2.5.2 and Section 2.5.3, respectively.

2.5.1. Heat transfer to the environment

In rotary dryers, thermal losses occur due to heat transfer through the shell to the environment. These heat losses are assigned to the gas phase, which is a common assumption in literature (Ajayi, 2011; Rousselet and Dhir, 2016). We choose the approach presented in Rousselet and Dhir (2016) adapted to an infinite-dimensional model

$$\dot{\gamma}_{loss}(t,x) = 22\pi D \left(\frac{\xi_a(t,x) v_{ma}(t,x)}{\pi D} \right)^{0.879} \left(T_{ma}(t,x) - T_{amb} \right), \tag{5}$$

where D is the dryer's diameter and T_{amb} the ambient temperature, which is assumed to be constant. This approach is chosen for two reasons. First, to calculate the heat transfer only geometry and process parameters are needed, which is advantageous to reduce the number of unknown variables as we limit ourselves to simulation studies in future work. Second, the approach is suitable for industrial-scale co-current rotary dryers and is applicable to a large range of dryer parameters (Rousselet and Dhir, 2016). If measurement data is available, it is also possible to apply the well-known approach for convective heat transfer, as shown in Section 2.5.2, where the local area for heat transfer is then given by the draft tube's perimeter.

2.5.2. Heat transfer between gas and particles

The heat transfer between the particle and the gas phase is considered to occur by convection. Hence, the local heat flow rate can be calculated as follows (Didriksen, 2002; Ajayi, 2011)

$$\dot{\gamma}_{\mathrm{conv}}(t,x) = \alpha_{\mathrm{conv}}(t,x) A_{\mathrm{conv}}(t,x) \left(T_{\mathrm{ma}}(t,x) - T_{\mathrm{mp}}(t,x)\right). \tag{6}$$

The variable $\alpha_{\mathrm{conv}}(t,x)$ denotes the heat transfer coefficient and $A_{\mathrm{conv}}(t,x)$ the contact surface between the particles and the gas. To determine the heat transfer coefficient, different approaches exist. On the one hand, it is modeled by means of an empirical relation depending on the mass flow rate of dry air (Rousselet and Dhir, 2016). On the other hand, the coefficient is calculated from Nusselts and Reynolds number (Didriksen, 2002; Ajayi, 2011). However, in some models the heat transfer coefficient is assumed to be constant (Rastikian et al., 1999; Ortega et al., 2007). The area available for heat transfer is either assumed to be equal to the surface area of the suspended particles (Didriksen, 2002), which is difficult to estimated (Ajayi, 2011), or is considered to be proportional to the mass of the solid phase (Ajayi, 2011). In this contribution we consider the heat transfer coefficient to be a function of the local mass flow rate of dry air. Moreover, we assume that the contact area between gas and particles is proportional to the mass flow rate of solid particles. This leads to

$$\begin{aligned}\dot{\gamma}_{\mathrm{conv}}(t,x) = k_{\mathrm{conv}} \left(\xi_{\mathrm{a}}(t,x) v_{\mathrm{ma}}(t,x)\right)^{k_{\mathrm{m}}} \left(\xi_{\mathrm{d}}(t,x) v_{\mathrm{mp}}(t,x)\right)^{k_{\mathrm{A}}} \\ \cdot \left(T_{\mathrm{ma}}(t,x) - T_{\mathrm{mp}}(t,x)\right),\end{aligned} \tag{7}$$

where $k_{\mathrm{conv}} > 0$, $k_{\mathrm{m}} > 0$ and $k_{\mathrm{A}} > 0$ are constant factors, which is similar to the approaches used in Arruda et al. (2009) and in Abbasfard et al. (2013).

2.5.3. Mass transfer due to evaporation

To model the evaporation rate in rotary dryers, two main approaches exist (Ajayi, 2011). With the first one, detailed drying kinetic models are derived from experiments (Arruda et al., 2009; Castaño et al., 2012). In the second one, the mass transfer is considered to be proportional to the difference of the partial pressure of water at the particle surface $p_{\mathrm{w}}(t,x)$ and that of vapor in the gas phase $p_{\mathrm{v}}(t,x)$ (Didriksen, 2002; Ajayi, 2011)

$$\dot{\mu}_{\mathrm{evap}}(t,x) = \beta(t,x) A_{\mathrm{evap}}(t,x) \left(p_{\mathrm{w}}(t,x) - p_{\mathrm{v}}(t,x)\right), \tag{8}$$

where $\beta(t,x)$ is the mass transfer coefficient and $A_{\mathrm{evap}}(t,x)$ the contact area between the particle and the gas phase. The partial pressure of water at the particle surface is calculated using (Didriksen, 2002)

$$p_{\mathrm{w}}(t,x) = \exp\left(27.468 - \frac{6580}{314 + T_{\mathrm{mp}}(t,x)}\right) \tag{9}$$

and that of vapor in the gas phase using Dalton's law. With this approach, the mass transfer coefficient is either assumed to be constant (Duchesne et al., 1997; Rastikian et al., 1999) or is calculated based on correlations (Didriksen, 2002), e.g. by the Chilton–Colburn analogy (Ajayi, 2011; Rousselet and Dhir, 2016). In the present contribution, we assume a constant proportionality factor between the heat and mass transfer coefficient. Furthermore, we assume that the contact area between gas and particles is the same as in the case of convection (Didriksen, 2002; Ajayi, 2011), so that we obtain the following equation

$$\begin{aligned}\dot{\mu}_{\mathrm{evap}}(t,x) = k_{\mathrm{evap}} \left(\xi_{\mathrm{a}}(t,x) v_{\mathrm{ma}}(t,x)\right)^{k_{\mathrm{m}}} \left(\xi_{\mathrm{d}}(t,x) v_{\mathrm{mp}}(t,x)\right)^{k_{\mathrm{A}}} \\ \cdot \left(p_{\mathrm{w}}(t,x) - p_{\mathrm{v}}(t,x)\right),\end{aligned} \tag{10}$$

where $k_{\mathrm{evap}} > 0$ is a constant factor.

2.6. Coupling of dryer and gas preparation unit

To determine the gas velocity $v_{\mathrm{ma}}(t,x)$ at the inlet of the dryer, the boundary conditions of the PDEs are inserted in (4), which yields

$$\begin{aligned}A = \left(\nu_{\mathrm{a}}(t,0)\dot{m}_{\mathrm{a,in}}(t) + \nu_{\mathrm{v}}(t,0)\dot{m}_{\mathrm{v,in}}(t)\right) / v_{\mathrm{ma}}(t,0) \\ + \nu_{\mathrm{d}}\dot{m}_{\mathrm{d,in}}(t) / \left(v_{\mathrm{rot}}(t) + k_{\mathrm{vel}} v_{\mathrm{ma}}(t,0)\right).\end{aligned} \tag{11}$$

When rearranging the equation w.r.t. $v_{\mathrm{ma}}(t,0)$, one obtains a quadratic equation for the unknown variable. As one solution is less or equal to zero for all $v_{\mathrm{rot}}(t) \geq 0$, the physical input velocity is uniquely defined by the previous equation. Having determined the input velocity, the mass densities at the inlet of the dryer can be calculated from the gas mass flows from the gas preparation unit using the boundary conditions specified in the respective PDE.

2.7. Implementation

To solve PDAE models, several approaches like special solvers (Lim et al., 2004) exist. However, such solvers are usually limited to certain classes of equations typically based on their index. A more recent approach (Lambert et al., 2020) is based on the reformulation of the PDAE as partial differential-relaxed equation (PDRE), where the algebraic constraint is approximated by means of a differential equation. This allows the application of a much broader range of methods and solvers. For the presented model, the corresponding differential equation of the algebraic constraint (4) is given by

$$\begin{aligned}&\partial_t \left(\nu_{\mathrm{d}}\xi_{\mathrm{d}}(t,x) + \nu_{\mathrm{a}}(t,x)\xi_{\mathrm{a}}(t,x) + \nu_{\mathrm{v}}(t,x)\xi_{\mathrm{v}}(t,x)\right) \\ &= -\kappa\left(A - \nu_{\mathrm{d}}\xi_{\mathrm{d}}(t,x) - \nu_{\mathrm{a}}(t,x)\xi_{\mathrm{a}}(t,x) - \nu_{\mathrm{v}}(t,x)\xi_{\mathrm{v}}(t,x)\right),\end{aligned} \tag{12}$$

where $\kappa > 0$. The newly obtained model can be solved for instance using a finite element solver like FENICS (Alnaes et al., 2015), where the previous equation might need to be transformed so that the spatial derivative of the velocity $v_{\mathrm{ma}}(t,x)$ appears explicitly in (12) by plugging in the PDEs (1)–(2). As an alternative, the Method of Lines is applicable to solve the PDRE. In general, the approach is quite similar to the well-known Baumgarte stabilization method for classical DAEs (Baumgarte, 1972).

3. Gas preparation unit model

To be able to provide flexibility while guaranteeing compliance with quality constraints, a model for the relation between the individual heat sources and the boundary conditions of the gas phase's PDEs is needed. According to van 't Land (2011), the drying gas is obtained by mixing secondary air into exhaust gases from a combustion chamber, which we will consider for modeling purposes as a sequence of a combustion and a mixing chamber. In the present paper, the combustion of natural gas $\dot{m}_{\mathrm{ng}}(t)$ with primary air $\dot{m}_{\mathrm{pa}}(t)$ is considered as the first heat source. The combustion gases $\dot{m}_{\mathrm{cc}}(t)$ are fed into the mixing chamber, where additional secondary air $\dot{m}_{\mathrm{sa}}(t)$ is supplied to control the temperature $T_{\mathrm{ma,in}}(t)$, mass flow of vapor $\dot{m}_{\mathrm{v,in}}(t)$ and dry gases $\dot{m}_{\mathrm{a,in}}(t)$ entering the dryer. In addition to the combustion chamber, we regard an electric heat source $\dot{Q}_{\mathrm{el}}(t)$, which allows for heating of the secondary air. Both, the temperature T_{amb} of the ambient air as well as its humidity, represented by the mass share of vapor $w_{\mathrm{v,amb}}$, are assumed to be constant. Analogous to the dryer model, we consider the gas flows to be composed of vapor and dry gases. For clarity, not all partial flows are shown in the scheme of the gas preparation unit in Fig. 5. In the following, the model assumptions are presented in Section 3.1. Afterwards, the mass and the energy balances are derived in Sections 3.2 and 3.3, respectively.

3.1. Gas preparation unit model assumptions

In this section, the assumptions from Section 2.1 are no longer applicable. Instead we consider the following ones

(l) the gas preparation unit is considered as a stationary process (Castaño et al., 2012)
(m) no heat losses to the environment occur (Castaño et al., 2012)
(n) the heat capacity of the dry combustion gas is equal to that of dry air

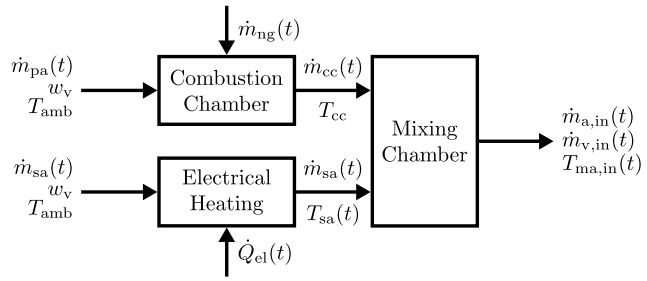

Fig. 5. Scheme of the gas preparation unit as parallel connection of a combustion chamber, fed with primary air $\dot{m}_{pa}(t)$ and natural gas $\dot{m}_{ng}(t)$, and a supply of secondary air $\dot{m}_{sa}(t)$ heated by electrical energy $\dot{Q}_{el}(t)$.

(o) temperature of the combustion gas is constant and equal to the adiabatic flame temperature of methane with air
(p) natural gas consists of nitrogen and methane, where w_{CH_4} is the mass fraction of methane (Hammer et al., 2006)
(q) pressure inside the gas preparation unit is constant (Langeheinecke et al., 2017)
(r) properties of mixtures are determined using linear mixing rules
(s) kinetic and potential energy of the gases are negligible.

Since gas preparation units are usually neglected in dryer models, we briefly discuss the most important assumptions. The overall process of gas preparation is considered to be a stationary process (l), i.e., its dynamic is assumed to be much faster compared to the dryer. This assumption is obviously true for the particle phase and can be considered reasonable for the gas phase because of the longer residence time due to the larger size and the presumably lower gas velocity compared to the gas preparation unit, which is also supported by Castaño et al. (2012). However, since the actual dimensions and shape of the gas preparation unit are not known it is not possible to estimate the heat losses, which motivates assumption (m) of an adiabatic unit. Assumption (n) may appear unintuitive as the composition of the gas changes due to the combustion. However, as significantly more ambient air than combustion gases are needed to obtain gas inlet temperatures typical for dryers (van 't Land (2011)) its specific heat capacity is primarily determined by the heat capacity of the ambient air. In Castaño et al. (2012) even the heat capacity of the overall combustion gas is considered to be equal to that of the ambient air, which neglects the high water fraction of the combustion gas. A further assumption (o) concerns the combustion process of the natural gas. Instead of determining the temperature of the combustion gases from an energy balance, the temperature is assumed to be constant and equal to the adiabatic flame temperature of methane. On the one hand, this is a simplification as the natural gas does not entirely consists of methane and the adiabatic flame temperature is a theoretical maximum temperature. On the other hand, this approach simplifies the adaption of the model to a real plant, since the adiabatic flame temperature can be easily replaced by a measured value of the combustion temperature. The remaining assumptions (p)–(s) are either verified by literature or have already been used in the dryer model, as shown in Section 2.1, and are thus not discussed in detail. Analogous to Section 2.1, we use the symbol T for the temperature in degree Celsius and choose 0 °C as the temperature reference point.

3.2. Mass balances of the gas preparation unit

Using assumption (l), the overall mass flow leaving the mixing chamber can be readily calculated from the sum of the supplied air and natural gas flows

$$\begin{aligned}\dot{m}_{a,in}(t) + \dot{m}_{v,in}(t) &= \dot{m}_{cc}(t) + \dot{m}_{sa}(t)\\ &= \dot{m}_{pa}(t) + \dot{m}_{ng}(t) + \dot{m}_{sa}(t).\end{aligned} \tag{13}$$

However, as the mass flow of dry air and vapor need to be known at the input of the rotary dryer model and for the calculation of the input temperature, the mass balances need to be evaluated separately for water vapor and dry air. Since the mass flow of methane or the related combustion energy can be seen as an input variable for process control, the mass flows related to the combustion are determined as a function of the natural gas mass flow. Equivalently, the mass flows of dry air and vapor related to the secondary air are determined as a function of the this overall flow. In the following, we denote the mass ratio of natural gas and dry primary air that is needed for a stoichiometric combustion, i.e., the stoichiometric air-to-fuel ratio, by $L_{a,e}$. Analogously, the mass flow of dry combustion gases is expressed as a multiple of the mass flow of natural gas denoted as $L_{a,p}$.

The overall mass flow of dry gas into the dryer is given by the sum of the inert gases contained in the dry primary air, the inert gases of the natural gas, the dry combustion gases and the dry air of the secondary air flow. Using the introduced abbreviations and assumptions (l), (p), this can be written as

$$\begin{aligned}\dot{m}_{a,in}(t) &= \dot{m}_{a,cc}(t) + \dot{m}_{a,sa}(t)\\ &= \left[L_{a,e}\left(1 - w_{O_2}\right) + \left(1 - w_{CH_4}\right) + L_{a,p}\right]\dot{m}_{ng}(t)\\ &\quad + \left(1 - w_v\right)\dot{m}_{sa}(t),\end{aligned} \tag{14}$$

where w_{O_2} denotes there mass fraction of oxygen in the dry ambient air. The vapor mass flow into the dryer is composed of the humidity related to the primary and secondary air flow and the water produced in the combustion. Thus, with assumptions (l), (p) one obtains the following equation for the vapor flow

$$\begin{aligned}\dot{m}_{v,in}(t) &= \dot{m}_{v,cc}(t) + \dot{m}_{v,sa}(t)\\ &= \left(L_{v,e} + L_{v,p}\right)\dot{m}_{ng}(t) + w_{v,amb}\dot{m}_{sa}(t).\end{aligned} \tag{15}$$

The term $L_{v,e}\dot{m}_{ng}(t)$ is the mass flow of vapor contained in the primary air and $L_{v,p}\dot{m}_{ng}(t)$ refers to the water vapor produced in the combustion, both expressed as a function of the natural gas flow.

3.3. Energy balances of the gas preparation unit

The combustion gases leaving the combustion chamber are assumed to have adiabatic flame temperature T_{cc}, which is taken from literature (Warnatz et al., 1996) for the combustion of methane with air. Under the assumptions (l)–(s), the energy flow out of the combustion chamber can be written with the previously introduced abbreviations

$$\begin{aligned}h_{cc}\dot{m}_{cc}(t) = h_{cc}\Big[&L_{v,e} + L_{v,p} + L_{a,p} + \left(1 - w_{CH_4}\right)\\ &+ L_{a,e}\left(1 - w_{O_2}\right)\Big]\dot{m}_{ng}(t),\end{aligned} \tag{16}$$

where h_{cc} is the enthalpy of the gas mixture with respect to the reference point. Different from the dryer model, the specific enthalpy of the pure components is calculated in this section using second-order polynomials as a function of the gas temperature where the coefficients are determined from literature data (Kretzschmar and Wagner, 2008; VDI e. V., 2013). This is necessary to accurately calculate the gas temperature due to the large temperature differences. For the specific enthalpy of a pure component, like dry air $h_{a,x}(t)$, one thus obtains a function of a temperature $T_x(t)$ of the form

$$h_{a,x}(t) = h_{a,2}T_x^2(t) + h_{a,1}T_x(t) + h_{a,0}. \tag{17}$$

Since the specific heat capacity of the dry combustion gas is assumed to be equal to that of the ambient air, the specific enthalpy of the gas mixture leaving the combustion chamber h_{cc} can be calculated from that of the pure components and the mass ratio of dry gases and water vapor. Considering assumptions (l), (m), (q)–(s), the energy balance of the secondary air flow is given by

$$h_{sa}(t)\dot{m}_{sa}(t) = h_{amb}\dot{m}_{sa}(t) + \dot{Q}_{el}(t), \tag{18}$$

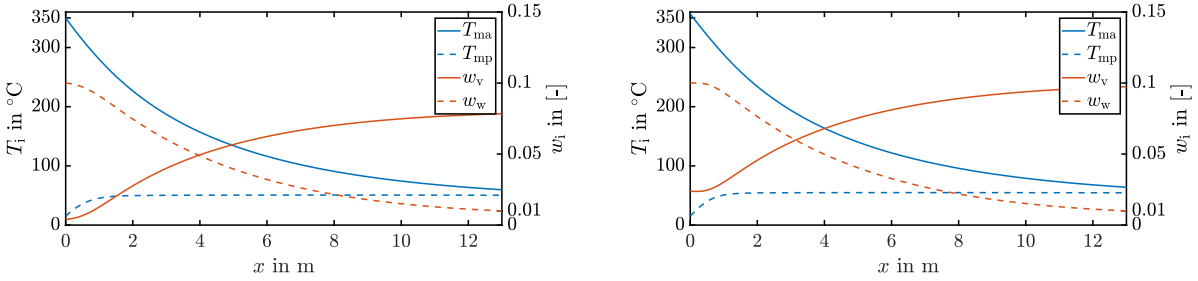

(a) Electrical heating. (b) Natural gas combustion.

Fig. 6. Temperature and humidity profiles of the particle and gas phase inside the dryer for different heat sources.

where h_{amb} is the specific enthalpy of the ambient moist air with respect to the reference point. Using the previous energy balances and assumptions (l)–(s), the energy balance of the moist air leaving the mixing chamber can be written as

$$h_{ma,in}(t)\dot{m}_{ma,in}(t) = h_{cc}\left[L_{a,p} + L_{v,p} + \left(1 - w_{CH_4}\right) + L_{a,e}\left(1 - w_{O_2}\right) + L_{v,e}\right]\dot{m}_{ng}(t) + h_{amb}\dot{m}_{sa}(t) + \dot{Q}_{el}(t). \tag{19}$$

The time-varying temperature $T_{ma,in}(t)$ of the moist gas flow can be determined by rearranging the previous equation using the specific enthalpy of the gas mixture

$$h_{ma,in}(t) = w_{a,ma,in}(t)h_{a,ma,in}(t) + w_{v,ma,in}(t)h_{v,ma,in}(t), \tag{20}$$

calculated from the mass shares of dry air $w_{a,ma,in}(t)$ and vapor $w_{v,ma,in}(t)$ in the moist air $\dot{m}_{ma,in}(t) = \dot{m}_{a,in}(t) + \dot{m}_{v,in}(t)$. However, since the transformed equation is lengthy, it is not shown in this contribution explicitly. Thus, all unknown boundary conditions of the moist air's PDEs (2) are determined and can be written as follows

$$\begin{bmatrix} \dot{m}_{a,in}(t) \\ \dot{m}_{v,in}(t) \\ T_{ma,in}(t) \end{bmatrix} = \begin{bmatrix} f_1(\dot{m}_{ng}(t), \dot{m}_{sa}(t)) \\ f_2(\dot{m}_{ng}(t), \dot{m}_{sa}(t)) \\ f_3(\dot{m}_{ng}(t), \dot{m}_{sa}(t), \dot{Q}_{el}(t)) \end{bmatrix}, \tag{21}$$

where $f_1(\cdot)$ is given by (14), $f_2(\cdot)$ by (15) and $f_3(\cdot)$ by (19) after the transformation w.r.t. the gas temperature.

4. Simulation and analysis

In the following, steady state simulation results of the proposed dryer model are presented for exemplary operating conditions of the Belite process. First, in Section 4.1, a qualitative comparison of the simulation results of the model based on a purely electrical energy supply with data and models from the literature is carried out. Afterwards, the effects of different types of flexibility on the process are investigated and conclusions are drawn on the required process control. In Section 4.2, switching to an energy supply by combustion is studied, while the variation of the throughput with unchanged energy sources is considered in Section 4.3. The geometric properties of the dryer are chosen according to van 't Land (2011), whereas the values of the heat and mass transfer coefficients are taken from Didriksen (2002) and Arruda et al. (2009). In order to allow for a comparison of the simulations for the different heat sources and throughputs, the input variables are adapted so that the final particle moisture is 1% and the gas temperature at the dryer's outlet is 10 K above the dew point temperature. Furthermore, the gas velocity at the inlet is limited to a maximum of 2 m s^{-1} (van 't Land, 2011). The choice of these reference variables is reasonable, since the final product moisture is the most important product property whereas the difference of the gas output temperature to the dew point temperature can be seen as a measure for the energy efficiency of the process (Blesl and Kessler, 2017). All input and output variables of the dryer simulation are summarized in Table 1, the used parameters are provided in Table 2.

4.1. Qualitative comparison

In Fig. 6(a) the temperature and humidity profiles inside the dryer are shown for purely electrical heating, where the most important characteristics are

- humidity profiles of the particle and the gas phase have an S-shaped form
- particle temperature increases close to the dryer inlet and stays approximately constant afterwards
- gas temperature monotonously decreases over the dryer length and has the shape of an exponentially decaying function.

These characteristics are typical for models and experimental data shown in literature, e.g. Ajayi (2011) and Rousselet and Dhir (2016). Due to this similarity to results of other works and measurement data, we consider our model to be plausible.

4.2. Change of heat supply

The simulation results using heat supply by combustion in Fig. 6(b) look quite similar to that obtained by electrical heating in Fig. 6(a) at first glace. However, there are a few differences. First, the gas input temperature is about 6 K and its humidity about two percentage points higher in case of the combustion. This can be explained by the production of water in the combustion process, which directly increases the vapor fraction in the gas flow, i.e. the gas is preloaded (van 't Land, 2011). Thus, a higher inlet temperature is needed to obtain the same particle humidity and temperature difference to the dew point at the dryer outlet. A second difference can be observed in the gas and particle humidity close to the inlet. For the combustion, the humidity stays constant for a short while before it starts to decrease like in case of the electrical heater, which is a consequence of the used evaporation approach. Due to the higher share of vapor in the combustion gases, the difference between the partial pressures is negative close to the dryer inlet, such that no water is vaporized (Kraume, 2020). Hence, the particles first heat up by a few degrees before the evaporation starts. The other process parameters like gas and particle velocities as well as their residence times are very similar for both simulations, as shown in Table 1.

In order to provide demand-side flexibility, the share of electrical energy in the energy supply must be at least partially replaced by the combustion of chemical energy sources during operation. To achieve this, one suitable approach is control allocation, where the inputs are changed in such a way that the controlled variables stay constant, i.e. acting in the shifted zero dynamics of the system (Johansen and Fossen, 2013). As an alternative, feedforward or flatness-based control could be used. Nevertheless, due to the relatively small differences between the input temperatures and mass flows of both simulations, it seems that it should be possible to switch slowly between the energy sources without any further control engineering measures in cases where only a small part of the electrical energy supply is replaced. Since an increasing

Table 1
Comparison of the process parameters for the use of different heat sources at nominal throughput and that of electrical heat supply at reduced throughput.

Variable	Electrical nominal	Combustion nominal	Electrical reduced	Unit
$\dot{m}_{\mathrm{ma,in}}$	1.75	1.74	1.89	kg s^{-1}
$\dot{m}_{\mathrm{ma,out}}$	1.89	1.88	2.01	kg s^{-1}
$\dot{m}_{\mathrm{mp,in}}$	1.56	1.56	1.24	kg s^{-1}
$\dot{m}_{\mathrm{mp,out}}$	1.42	1.42	1.13	kg s^{-1}
$T_{\mathrm{ma,in}}$	350	356.01	276.68	°C
$T_{\mathrm{ma,out}}$	59.71	63.20	55.53	°C
$T_{\mathrm{mp,in}}$	15	15	15	°C
$T_{\mathrm{mp,out}}$	50.46	53.86	45.70	°C
$v_{\mathrm{ma,in}}$	1.92	1.94	1.80	m s^{-1}
$v_{\mathrm{ma,out}}$	1.17	1.18	1.19	m s^{-1}
$v_{\mathrm{mp,in}}$	0.0083	0.0083	0.0081	m s^{-1}
$v_{\mathrm{mp,out}}$	0.0071	0.0072	0.0072	m s^{-1}
$w_{\mathrm{ma,in}}$	0.004	0.020	0.004	–
$w_{\mathrm{ma,out}}$	0.078	0.094	0.060	–
$w_{\mathrm{mp,in}}$	0.1	0.1	0.1	–
$w_{\mathrm{mp,out}}$	0.01	0.01	0.01	–
τ_{ma}	9.64	9.54	9.63	s
τ_{mp}	29.05	29.00	29.07	min

Table 2
Further parameters used in all simulations.

Parameter	Value	Unit
c_{d}	0.88	kJ (kg K)$^{-1}$
c_{w}	4.2	kJ (kg K)$^{-1}$
$c_{\mathrm{p,a}}$	1.05	kJ (kg K)$^{-1}$
$c_{\mathrm{p,v}}$	2.08	kJ (kg K)$^{-1}$
D	1.5	m
k_{A}	0.541	–
k_{conv}	190	–
k_{evap}	$0.2{\cdot}10^{-5}$	–
k_{m}	0.6	–
k_{vel}	0.0015	–
ℓ	13	m
$L_{\mathrm{e,a}}$	16.71	–
$L_{\mathrm{e,v}}$	0.07	–
$L_{\mathrm{p,a}}$	2.66	–
$L_{\mathrm{p,v}}$	2.18	–
p	$1 \cdot 10^5$	Pa
T_{amb}	15	°C
T_{cc}	1949	°C
v_{rot}	0.005	m s^{-1}
$w_{\mathrm{CH_4}}$	0.97	–
$w_{\mathrm{O_2}}$	0.23	–
ν_{d}	1/1400	m^{-3} kg

share of combustion gases results in a higher vapor content in the input stream, the differences for higher inlet temperatures are expected to be more significant. It should be noted that it was not possible to find a new operating point matching both the desired particle humidity and the desired difference to the dew point while meeting the constraint to the gas velocity. Thus, as final product moisture is assumed to be the more important process output, a new operating point where the temperature difference is close to 10 K is considered. This might lead to several possible operating points of comparable suitability. Thus, the velocity restriction also forces a change of the reference value of the desired temperature difference. However, this aspect needs to be further investigated.

4.3. Change of throughput

To investigate the impact of the change of the material throughput, a reduction of the feed stream to 80% of the nominal capacity is regarded. From Fig. 7 it can seen that the temperature and humidity profiles are of a similar shape as with electrical heat supply at nominal throughput. However, the mass flow of gas and its temperature change significantly as due to reduced throughput less water needs to be

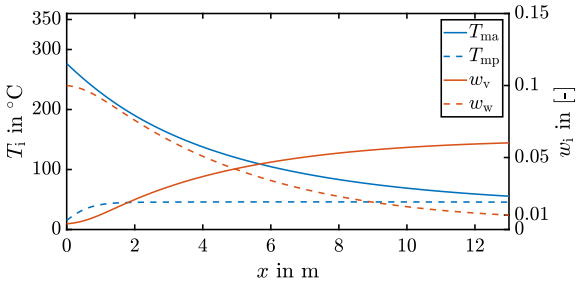

Fig. 7. Temperature and humidity profiles of the particle and gas phase inside the dryer for a reduced material throughput and electrical heating.

evaporated and consequently less energy needs to be supplied via the gas stream. Whereas the input temperatures reduces by about 74 K, the mass flow of the hot gas stream towards the dryer increases slightly as shown in detail in Table 1. Thus, in order to provide flexibility with a short response while continuously meeting the product requirements, precise feedforward control is needed. Similar to the case of the variation of the energy source, a slight change of the desired temperature difference is necessary to meet the constraint according to the model.

5. Conclusion and outlook

The contribution presents a new control-oriented model for co-current rotary dryers based on partial differential-algebraic equations. Its development is motivated by the lack of suitable distributed parameter models, which are needed for the development of new control concepts for demand-side flexibility. The latter is regarded as an important aspect in the energy transition.

The presented model is the first purely distributed parameter model that considers both spatially dependent gas and particle velocities as well as interactions between the phases in particle transport. The particle velocity is modeled as a function of a purely time-dependent as well as a time- and location-dependent velocity component, where the latter is considered to be proportional to the local gas velocity. This approach is motivated by residence time models, existing theoretical work on particle transport and a previously introduced velocity approach for concentrated parameter models. The new dryer model also differs from most other distributed parameter models by the comparatively complex approaches modeling heat and mass exchange between the phases. In combination with the new particle transport approach, this should allow for a wide range of validity of the model, which is necessary for the development of control concepts for demand-side flexibility. Within the contribution two flexibility mechanisms, the variation of throughput as well as the change of energy source, are considered. To allow for the investigation of the latter, also a model of a heat supply unit is developed.

It is shown by simulation that the stationary solution of the proposed model coincides with other models published in literature and measurement data. For this reason, the developed model is considered to be plausible. By choosing suitable output variables that allow for the comparison of the different simulations, the effect of the flexibility mechanisms on temperature and humidity profiles inside the dryer is investigated. Moreover, implications for process control w.r.t. the usage of control concepts like control allocation and feedforward control are discussed. The simulations show that especially the variation of the material throughput requires a significant change in the gas inlet temperature and mass flow, which necessitates the use of advanced process control. Furthermore, it is found that the desired outlet gas temperature may need to be varied when providing flexibility in order to meet process-side constraints.

In an upcoming work, we will include a PDE for the shell temperature to the model and investigate whether this has significant effects

Table 3
Symbol and subscript nomenclature.

Symbol		Unit
A	Cross sectional area	m^2
c	Specific heat capacity	J $(kg\ K)^{-1}$
c_p	Specific isobaric heat capacity	J $(kg\ K)^{-1}$
D	Diameter	m
f	General function	–
h	Specific enthalpy	J kg^{-1}
Δh_v	Specific enthalpy of evaporation	J kg^{-1}
k	Proportionality factor	–
ℓ	Length of the dryer	m
L	Proportionality factor between natural gas flow and reaction educts or products for stoichiometric combustion	–
$\dot{m}$	Mass flow	kg s^{-1}
$\dot{Q}$	Heat flow	W
T	Temperature	°C
v	Velocity	m s^{-1}
w	Mass fraction $w_i = \xi_i / \sum \xi_j$	–
α	Heat transfer coefficient	W $(m^2\ K)^{-1}$
$\dot{\gamma}$	Heat flow density	J $(s\ m)^{-1}$
$\dot{\mu}$	Mass flow density	kg $(s\ m)^{-1}$
ν	Specific volume	$m^3\ kg^{-1}$
ξ	Linear mass density	kg m^{-1}
τ	Residence time	s or min
Subscript		
a	Dry air	
amb	Ambient conditions	
cc	Combustion chamber	
conv	Heat exchange between gas and particles	
d	Dry particles	
e	Combustion educt	
el	Electrical	
evap	Evaporation	
in	Dryer inlet	
loss	Heat exchange between gas and environment	
ma	Moist air	
meth	Methane	
mp	Moist particles	
ng	Natural gas	
out	Dryer outlet	
p	Combustion product	
pa	Primary air	
sa	Secondary air	
v	Water vapor	
w	Liquid water	

on the steady-state and transient behavior of the model. Moreover, we will deal with possible model simplifications for easier controller development and design a new control concept on the basis of this model with a focus on energy efficiency and flexibility.

Funding

This work was supported by the Helmholtz Association, Germany under the Innopool Project “Energy Transition and Circular Economy”.

CRediT authorship contribution statement

Jan M. Schaßberger: Methodology, Writing – original draft, Writing – review & editing, Visualization, Software. **Lutz Gröll:** Conceptualization, Supervision, Methodology. **Veit Hagenmeyer:** Conceptualization, Funding acquisition, Supervision.

Declaration of competing interest

The authors declare that they have no known competing financial interests or personal relationships that could have appeared to influence the work reported in this paper.

Data availability

No data was used for the research described in the article.

References

Abbasfard, H., Rafsanjani, H., Ghader, S., Ghanbari, M., 2013. Mathematical modeling and simulation of an industrial rotary dryer: A case study of ammonium nitrate plant. Powder Technol. 239, 499–505.
Ajayi, O., 2011. Multiscale Modelling of Industrial Flighted Rotary Dryers (Ph.D. thesis). James Cook University.
Alnaes, M.S., Blechta, J., Hake, J., Johansson, A., Kehlet, B., Logg, A., Richardson, C., Ring, J., Rognes, M.E., Wells, G.N., 2015. The FEniCS project version 1.5. Arch. Numer. Softw. 3 (100), 9–23.
Arruda, E., Lobato, F., Assis, A.J., Barrozo, M., 2009. Modeling of fertilizer drying in roto-aerated and conventional rotary dryers. Drying Technol. 27 (11), 1192–1198.
Baker, C., 1992. Air-solids drag in cascading rotary dryers. Drying Technol. 10, 365–393.
Baumgarte, J., 1972. Stabilization of constraints and integrals of motion in dynamical systems. Comput. Methods Appl. Mech. Engrg. 1 (1), 1–16.
Blesl, M., Kessler, A., 2017. Energieeffizienz in der Industrie (Energy Efficiency in the Industry) second ed. Springer Vieweg.
Castaño, F., Rubio, F., Ortega, M., 2012. Modeling of a cocurrent rotary dryer. Drying Technol. 30, 839–849.
Cruz, M., Fitiwi, D., Santos, S., Catalão, J., 2018. A comprehensive survey of flexibility options for supporting the low-carbon energy future. Renew. Sustain. Energy Rev. 97, 338–353.
Delele, M., Weigler, F., Mellmann, J., 2015. Advances in the application of a rotary dryer for drying of agricultural products: A review. Drying Technol. 33 (5), 541–558.
Deutscher, J., 2012. Zustandsregelung verteilt-parametrischer Systeme. (State Control of Distributed Parameter Systems) Springer.
Didriksen, H., 2002. Model based predictive control of a rotary dryer. Chem. Eng. J. 86 (1), 53–60, Drying 2000: Selected Papers from the 12th International Symposium IDS2000.
Duchesne, C., Thibault, J., Bazin, C., 1997. Modelling and dynamic simulation of an industrial rotary dryer. Dev. Chem. Eng. Miner. Process. 5 (3–4), 155–182.
Föllinger, O., 2016. Regelungstechnik: Einführung in die Methoden und ihre Anwendung (Control Engineering: Introduction to the Methods and their Application) twelfth ed. VDE Verlag,
Hammer, G., Lübcke, T., Kettner, R., Pillarella, M., Recknagel, H., Commichau, A., Neumann, H.-J., Paczynska-Lahme, B., 2006. Natural gas. In: Ullmann’s Encyclopedia of Industrial Chemistry. John Wiley & Sons, Ltd.
Heffron, R., Körner, M.F., Wagner, J., Weibelzahl, M., Fridgen, G., 2020. Industrial demand-side flexibility: A key element of a just energy transition and industrial development. Appl. Energy 269, 115026.
Johansen, T., Fossen, T., 2013. Control allocation – A survey. Automatica 49 (5), 1087–1103.
Kamke, F., 1983. Engineering Analysis of a Rotary Dryer: Drying of Wood Particles (Ph.D. thesis). Oregon State University.
Kraume, M., 2020. Transportvorgänge in der Verfahrenstechnik (Transport Processes in Process Engineering) third ed. Springer Vieweg.
Kretzschmar, H.-J., Wagner, W., 2008. International Steam Tables, third ed. Springer Vieweg.
Lambert, W., Alvarez, A., Ledoino, I., Tadeu, D., Marchsein, D., Bruining, J., 2020. Mathematics and numerics for balance partial differential-algebraic equations (PDAEs). J. Sci. Comput. 84, 29.
van ’t Land, C., 2011. Drying in the Process Industry. Wiley.
Langeheinecke, K., Kaufmann, A., Langeheinecke, K., Thieleke, G., 2017. Thermodynamik für Ingenieure (Thermodynamics for Engineers) tenth ed. Springer Vieweg.
Leipold, J., Seidel, C., Nikolic, D., Seidel-Morgenstern, A., Kienle, A., 2023. Optimization of methanol synthesis under forced periodic operation in isothermal fixed-bed reactors. Comput. Chem. Eng. 175, 108285.
Lim, Y.I., Chang, S.C., Jørgensen, S., 2004. A novel partial differential algebraic equation (PDAE) solver: Iterative space–time conservation element/solution element (CE/SE) method. Comput. Chem. Eng. 28 (8), 1309–1324.
Morris, K., 2020. Controller Design for Distributed Parameter Systems. Communications and Control Engineering, Springer Nature.
Mujumdar, A. (Ed.), 2007. Handbook of Industrial Drying, third ed. A CRC Press Book, CRC, Taylor & Francis.
Ortega, M., Castaño, F., Vargas, M., Rubio, F., 2007. Multivariable robust control of a rotary dryer: Analysis and design. Control Eng. Pract. 15 (4), 487–500.
Otashu, J., Baldea, M., 2019. Demand response-oriented dynamic modeling and operational optimization of membrane-based chlor-alkali plants. Comput. Chem. Eng. 121, 396–408.
Perazzini, H., Freire, F., Freire, J., 2014. Prediction of residence time distribution of solid wastes in a rotary dryer. Drying Technol. 32 (4), 428–436.

Rastikian, K., Capart, R., Benchimol, J., 1999. Modelling of sugar drying in a countercurrent cascading rotary dryer from stationary profiles of temperature and moisture. J. Food Eng. 41, 193–201.
Rosbo, J., Ritschel, T., Hørsholt, S., Huusom, J., Jørgensen, J., 2023. Flexible operation, optimisation and stabilising control of a quench cooled ammonia reactor for power-to-ammonia. Comput. Chem. Eng. 176, 108316.
Rousselet, Y., Dhir, V., 2016. Numerical modeling of a co-current cascading rotary dryer. Food Bioprod. Process. 99, 166–178.
Silva, M., Lira, T., Arruda, E., Murata, V., Barrozo, A., 2012. Modelling of fertilizer drying in a rotary dryer: Parametric sensitivity analysis. Braz. J. Chem. Eng. 29 (2), 359–369.
Stemmermann, P., Ullrich, A., Beuchle, G., Garbev, K., Schweike, U., 2022. Belite cement clinker from autoclaved aerated concrete waste – A contribution towards CO2-reduced circular building materials. ce/papers 5 (5), 17–26.
Thibault, J., Alvarez, P., Blasco, R., Vega, R., 2010. Modeling the mean residence time in a rotary dryer for various types of solids. Drying Technol. 28 (10), 1136–1141.
Tsotsas, E., Mujumdar, A. (Eds.), 2012. Modern Drying Dechnology, Vol. 4: Energy Savings. Wiley-VCH.
VDI e. V. (Ed.), 2013. VDI-Wärmeatlas (VDI Heat Atlas) eleventh ed. Springer Vieweg.
Warnatz, J., Maas, U., Dibble, R., 1996. Combustion: Physical and Chemical Fundamentals, Modelling and Simulation, Experiments, Pollutant Formation. Springer.
Wei, M., McMillan, C., de la Rue du Can, S., 2019. Electrification of industry: Potential, challenges and outlook. Curr. Sustain./Renew. Energy Rep. 6, 140–148.
Weigert, J., Hoffmann, C., Esche, E., Fischer, P., Repke, J.U., 2021. Towards demand-side management of the chlor-alkali electrolysis: Dynamic modeling and model validation. Comput. Chem. Eng. 149, 107287.
Yliniemi, L., 1999. Advanced Control of a Rotary Dryer (Ph.D. thesis). University of Oulu.